Design and implementation of an optimized mask RCNN model for liver tumour prediction and segmentation

Thakur, Raman; Volety, Dayal Rohan; Sharma, Vandana; Mishra, Sushruta; Iwendi, Celestine; Osamor, Jude

Published in:
Proceedings of ICCAKM 2023: 4th International Conference on Computation, Automation and Knowledge Management

DOI:
10.1109/ICCAKM58659.2023.10449653

Publication date:
2024

Document Version
Author accepted manuscript

Design and Implementation of an Optimized Mask RCNN Model for Liver Tumour Prediction and Segmentation

Raman Thakur
Kalinga Institute of Industrial Technology, Deemed to be University,
Bhubaneswar,India
20051900@kiit.ac.in

Dayal Rohan Volety
Kalinga Institute of Industrial Technology, Deemed to be University,
Bhubaneswar,India
2005630@kiit.ac.in

Vandana Sharma
Department of Computational Sciences, CHRIST (Deemed to be University),
Delhi NCR, India
vandana.juyal@gmail.com

Sushruta Mishra
Kalinga Institute of Industrial Technology, Deemed to be University,
Bhubaneswar,India
sushruta.mishrafcs@kiit.ac.in

Celestine Iwendi, SMIEEE
School of Creative Technologies
University of Bolton, United Kingdom
c.iwendi@bolton.ac.uk

Jude Osamor, FHEA
Department of Cybersecurity and Networks
Glasgow Caledonian University
Glasgow, G4 0BA Scotland, UK
jude.osamor@gcu.ac.uk

***Abstract*—Liver tumour segmentation is a challenging task due to the wide diversity in size, position, depth, and proximity to surrounding organs. This research uses the state-of-the-art model of Mask R-CNN model with the ResNet-50 architecture as the backbone. The suggested methodology leverages the Mask Region-Convolutional Neural Network approach to accurately identify liver tumors by identifying tumour location. To address variations of the liver and CT scan images with different parameters. The normalized CT images are then fed into the RESNET-50 model to extract relevant features. Subsequently, the liver tumor are segmented using the Mask R-CNN algorithm. The experimental dataset used in this study consists of one hundred and thirty CT scans obtained from various hospitals and nursing homes, which are freely accessible on the LiTS web page. The suggested algorithm is trained on transformed CT image slices. The results demonstrate that the proposed Mask RCNN system, with its innovative connections, surpasses state-of-the-art methods in identifying liver tumor, achieving a remarkable DSC value of 0.97%. This technique has the potential to significantly contribute to early and precise diagnosis of liver tumor in the field of biotechnology, potentially saving many patients' lives.**

Keywords—Liver Tumour segmentation, Machine learning, CT-Image, convolution neural network, Mask RCNN

I. INTRODUCTION

Abnormal growths or lumps that form within the liver tissue are referred to as liver tumor. They may be malignant (cancerous) and benign (non-cancerous). Hepatocellular carcinoma (HCC), another name for liver cancer, is the primary liver cancer type and is mainly responsible for a sizable portion of cancer-oriented casualties worldwide.

Liver tumor start to grow for several reasons, including alcohol abuse, cirrhosis, chronic liver illnesses including hepatitis B or C, and also due to specific hereditary abnormalities. The result of metastasis, where cancer cells from other regions of the body travel to the liver, can also take place.

Detection and correct identification of liver tumor at an early stage is necessary for efficient treatment and better patient outcomes. For the diagnosis, characterization, and staging of liver tumor various scans are done to collect the patient's liver images. Planning and managing treatment are made easier by the extensive information these imaging modalities provide on the tumor' dimensions, locations, and features. The variety of appearances and traits that liver tumor might exhibit makes it very difficult to distinguish them from the surrounding healthy liver tissue. For the detection and diagnosis of liver tumor, radiologists and oncologists rely heavily on their experience and also on visual evaluation of medical imaging. Manual detection of these images is time-consuming, subjective, and highly sensitive to human error. The topic of medical imaging and detecting liver tumor underwent a huge revolution due to the development of novel deep-learning methods. Deep learning models and advanced algorithms have been created and used by researchers to detect and segment liver tumor. These methods make use of the power of artificial intelligence to analyze medical images, and to give accurate tumour delineation. Mask R-CNN is one cutting-edge deep learning system that combines object detection along with instance segmentation abilities.

This paper aims to to provide a unique method for using a mask R-CNN to identify and segment liver tumour through various CT scans. The goal is to create an effective system that can automatically identify liver tumor and produce a pixel-level segmentation by using the advantages of this sophisticated deep learning architecture. The Mask R-CNN model is trained as part of the research technique using a big dataset of liver CT scans. The proposed model can generalize successfully to various liver tumour scenarios through a thorough annotation process and data augmentation strategies. To calculate the precision and robustness of the research model, various criteria are taken into account like precision, recall, Dice coefficient, and intersection over union (IoU).

The outcomes of this study have important ramifications in the detection and treatment of liver cancer. Radiologists and oncologists also benefit from the creation of an automated liver tumour detection and segmentation system employing the novel Mask RCNN model for early and quick image processing.

Major Highlights of the paper are as follows:

- The paper proposes a liver tumour detection model using the Mask RCNN to detect the tumor of the liver.

- The proposed model makes use of ResNet architecture, which simplifies the structure of the model's layers to detect tumor effectively..
- Adjustments are made to the ResNet architecture's layers to give better accuracy than all the existing models.

II. Literature Review

For the identification and detection of liver and liver contusion, authors in [1] developed a cascaded fully convolutional neural network (FCN) strategy along with 3D conditional random fields (CRFs). On a dataset of abdominal CT images, they were successful in accurately segmenting the data. For autonomous liver tumour segmentation in CT scans, the scientists [2] presented a deep learning-based method employing a fully convolutional neural network (FCN). Their technique demonstrated its promise for clinical applications by segmenting liver tumor with a high degree of precision. To segment liver tumor in CT scans, authors in [3] presented a multi-modal transfer learning framework along with deep convolutional neural networks (CNNs). By utilizing both linked MRI scans and CT images, they were able to produce precise segmentation results, improving the efficiency of liver tumour identification. In [4], deep convolutional neural networks with uncertainty estimates to segment liver tumor. The authors put forth a probabilistic U-Net architecture, showed how effective it was at accurately segmenting tumor, and provided uncertainty maps to gauge the accuracy of results. In the study, a method for automatically segmenting liver tumor in MRI images using convolutional neural networks (CNN) was introduced. Their [5] approach produced precise tumour segmentation results, showing the promise of deep learning in MRI-based liver tumour analysis. This study is focused on utilizing deep convolutional neural networks (DNNs) in the detection of liver tumor in various CT scans. The aim is to show the capability of deep learning techniques in identifying various tumour detection. By using CNNs, which are capable of learning hierarchical features from image data, this study is aimed to develop a reliable and automated approach for tumour detection in CT scans, the scientists [6] created a CNN-based model that successfully achieved high accuracy in detecting liver tumor. A segmentation model based on triplane views, including axial, sagittal, and coronal plane axes, was proposed by the authors in [7]. The con-vNet model receives input from this network of connected planes. To detect liver tumor from CT scans, [8] suggest a hybrid deep learning strategy that blends convolutional neural networks (CNN) and recurrent neural networks (RNN). With the identification of liver tumor from Computed Tomography Scan images, authors in [9] offer an approach that blends deep learning methods with the Hough transform. The fuzzy C-means clustering approach suggested by work in [10] is used in the detection of tumor using dynamic contrast-enhanced MRI. Researchers have utilized various machine learning techniques to distinguish between tumor and the liver over the decade. Using local and global energy functions in a level-set approach is the second step in [11] autonomous 3D liver segmentation strategy. The first step is to detect the initial liver border using the total variation with the L1 norm (TV-L1). For more precise segmentation, a texture analysis technique based on the grey-level co-occurrence matrix (GLCM) is applied. For the automatic segmentation of abdominal organs, including the liver, study in. [12] presented the level estimation (SIMPLE) approach based on multi-atlas segmentation (MAS). A fully automatic adaptive FMM-based liver segmentation algorithm was created by authors in [13]. The suggested adaptive FMM makes use of self-adaptive parameter adjustment. The intensity statistics of the potential liver region on computed tomography (CT) slices can be used to estimate the size of the liver region. By analyzing the intensity values within the region of interest, various statistical measures such as mean, standard deviation, median, or percentile values can be calculated., the arrival time is modified in FMM. Work in [14] used CT scans that made use of abdominal artery channels at the entrance stage to build a semi-automated technique for fragmenting the hepatic low-intensity tumour. [15] proposed a finite difference energy method that incorporates factors such as brightness, region attractiveness, and surface smoothing. This method aims to enhance the accuracy and effectiveness of image-processing tasks by considering these important aspects.

III. PROPOSED METHODOLOGY

The Mask RCNN architecture is a better alternative to the faster RCNN, RCNN, and fast RCNN designs The Mask RCNN is an extension and improvement of the Faster RCNN architecture. It builds upon the foundation of Faster RCNN and introduces an additional branch for pixel-level segmentation, making it an all-inclusive conceptual framework [16].

The Mask R-CNN incorporates an extra branch dedicated to segmenting masks for all the regions that are of interest. In contrast, the Faster RCNN architecture comprises branches that are dedicated to classification and bounding box regression tasks. However, the Mask RCNN introduces an extra branch known as the mask branch. In this branch, a smaller complete CNN layer(FCN) is applied to each region of interest (RoI) to predict the pixel-level segmentation mask [17].

The Mask R-CNN improves the functionalities of the Faster R-CNN by introducing bounding box localization and classification. It incorporates a region proposal network (RPN) to extract relevant features. The Mask R-CNN employs the concept of maximum convergence to handle multi-scale RoI features effectively. To achieve this, it utilizes the RoIAlign layer as a substitute for the RoIPool layer used in Faster R-CNN for feature extraction, RoI quantification, and handling. The RoIAlign layer enables precise localization of object regions labeled with masks in the Mask RCNN. The following equation 1 shows loss function formulation can be used with the Mask R-CNN for multitask learning.

$$L = L_{class} + L_{bbox} + L_{mask} \quad (1)$$

As shown in equation (2) Lclass+Lbox are coming from faster RCNN framework, here Lbox describes the localization of object bounding boxes.

$$L_{cls} + L_{box} = \frac{1}{Ncls}\sum_i L_{cls}(p_i, p_i^*) + \frac{1}{Nbox}\sum_i^n p_i^* L_1^{smoot}\ (t_i - t_i^*) \quad (2)$$

Equation (3) shows Lclass which is defined as classification loss based on the target's segmentation requirements.

$$L_{cls}(\{p_i, p_i^*\}) = -p_i^* log p_i^* - (1 - p_i^*) log(1 - p_i^*) \quad (3)$$

and equation (4) shows Lmask which is known as the average binary cross-entropy loss:

$$L_{mask} = -\frac{1}{m^2}\sum_{1\le i.j\le m}[y_{ij} log\ o\ y_{ij}^k + (1 - y_{ij}) log(1 - o y_{ij}^k)] \quad (4)$$

A. Improved Mask R-CNN

In the upgraded Mask R-CNN, the model undergoes multiple training rounds, which allows it to learn specific characteristics of liver and images. As the training progresses,

the prediction box parameters are adjusted to closely align them with the ground truth box values, by enhancing convergence and precision of liver identification and segmentation. The goal is to improve the localization accuracy and the segmentation precision for liver-related tasks using the existing Mask R-CNN framework [18].

Typically, the backbone network of Mask RCNN utilizes ResNet50 as its base architecture. ResNet50 refers to a Residual Network with 50 layers,However, employing too many layers in the network structure can potentially lead to issues such as vanishing gradients or increased computational complexity. The Liver tumour detection model developed in this article is quite basic, and the network layer needs are reduced; consequently, ResNet50 is used to increase the algorithm's running speed.

Because the tumour sizes in the photos will vary, a single CNN cannot pull out all of the image features adequately. As shown in Fig 1. in this research paper, the backbone 2) Region proposal Network

As shown in the figure in Fig 3, mask R-CNN architecture uses the region proposal network which has been utilized in this study. Shallow characteristics can help identify objects while deeper features are more effective, in distinguishing targets. The RPN receives feature maps of sizes generated by the FPN. It is common to select the region of interest (ROI) before segmenting an image. This is because some photos are more intricate than others making it challenging to segment the image and obtain accurate segmentation results. However, with a candidate box, the difficulty of segmentation can be significantly reduced. The network adjusts its scale based on the input images. Incorporates a set of predetermined anchor boxes. These anchor boxes define the bounding boxes and corresponding classes, with ground truth information each given a unique anchor.architecture of ResNet50, a popular deep convolutional neural network, is utilized as the foundational structure. ResNet50 has proven to be effective in various computer vision tasks due to its deep architecture [19].

With the help of FPN, The Mask R-CNN addresses the challenge of extracting target objects from photos at multiple scales by employing a top-down hierarchy approach with lateral connections, the Mask RCNN architecture begins with a single-scale input and gradually constructs a network feature pyramid. This feature pyramid is designed to capture and incorporate information at multiple scales. This enables the model to effectively handle objects of varying sizes and achieve accurate segmentation results.This structure needs fewer parameters and is adaptable [20].

The enhanced ResNet structure provides two major benefits when the layers are adjusted on the residual branch. First is ,the back-propagation essentially satisfies the criteria, and According to Fig. 2, the FPN consists of lateral connections and a top-down and bottom-up pathway. Convolutional neural networks ResNet50, are used for feature extraction in the bottom-up approach. The spatial dimension is halved and the stride is increased by two. Each convolutional layer uses the label sent through the top-down route. FPN also builds the higher resolution layers from a semantically rich layer in a top-down route. Later, there is the addition of lateral connections between the reconstructed layers and the relevant feature maps to aid the detector in accurately predicting the position.

Data flow is unchanged. Second aspect is that Batch Normalization (BN) layer acts as a pre-activation layer, where "pre" is referring to the weight layer. This configuration of the BN layer also improves the regularization and the overall generalization of the model.

B. Mask RCNN

There are two distinct stages in a Mask RCNN mode. Based on the provided image, it creates region proposals where an object might be. Based on the first stage proposal, it then convinces the object's class, fine-tunes the b-box, and applies a colour mask at the pixel level of the item. Both stages are joined by a backbone structure [21].

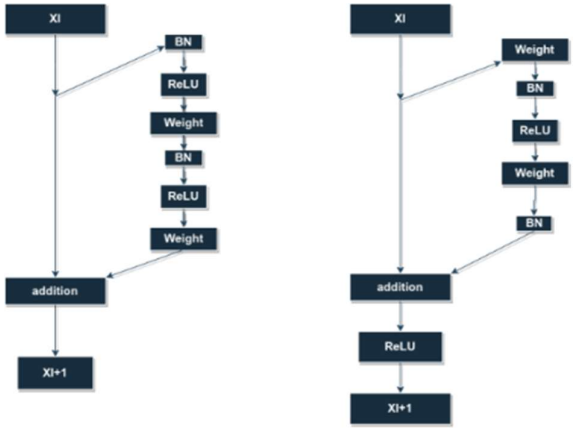

Fig 1. Improved ResNet vs ResNet Structure

C. The architecture of Improved Mask RCNN

1) Feature Pyramid Network

FPN is a feature extractor method generated to quickly as well as accurately achieve such pyramid notions. According to RPN, FPN extracts feature maps and then feeds them into a detector for object detection. In order to anticipate if each location has an item and its border box, RPN uses a sliding window over the feature maps. It takes the place of Mask RCNN's feature extractor and produces multi-scale feature maps for object detection that contain standard information than the standard feature pyramid. According to Fig. 2, the FPN consists of lateral connections and a top-down and bottom-up pathway. Convolutional neural networks ResNet50, are used for feature extraction in the bottom-up approach. The spatial dimension is halved and the stride is increased by two. Each convolutional layer uses the label sent through the top-down route.FPN also builds the higher resolution layers from a semantically rich layer in a top-down route. Later, there is the addition of lateral connections between the reconstructed layers and the relevant feature maps to aid the detector in accurately predicting the position.

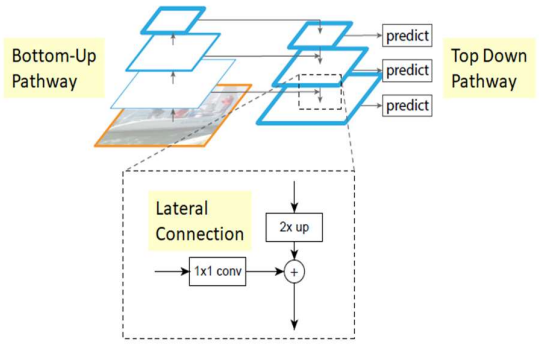

Fig 2. Feature Pyramid Network Backbone

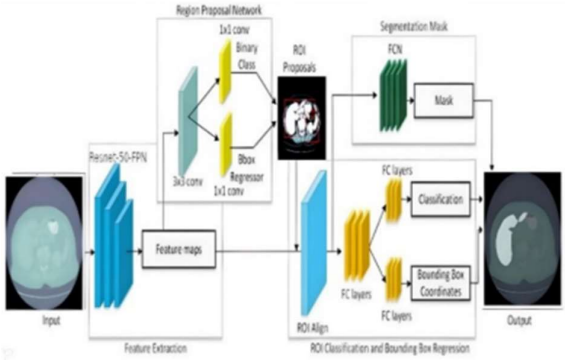

Fig 3. Improved Mask RCNN architecture

2) Region proposal Network

As shown in the figure in Fig 3, mask R-CNN architecture uses the region proposal network which has been utilized in this study. Shallow characteristics can help identify objects while deeper features are more effective, in distinguishing targets. The RPN receives feature maps of sizes generated by the FPN. It is common to select the region of interest (ROI) before segmenting an image. This is because some photos are more intricate than others making it challenging to segment the image and obtain accurate segmentation results. However, with a candidate box, the difficulty of segmentation can be significantly reduced. The network adjusts its scale based on the input images. Incorporates a set of predetermined anchor boxes. These anchor boxes define the bounding boxes and corresponding classes, with ground truth information each given a unique anchor. For each of the anchors, RPN suggests two outputs: bounding box parameters and the anchor class. as seen in Fig. 4. To find RoI, RPN applied several anchors to the picture and then gave confidence scores for each location. To recognize tumor of various sizes and shapes, default bounding boxes come in a range of sizes and aspect ratios. These boxes overlap one another numerous times, making it easier to choose the greatest confidence score. As shown in equation 5, to calculate the IoU, the intersection area between the predicted box and the ground truth box is divided by the union area of the two boxes. Greater alignment between the expected and ground truth regions is indicated by a higher IoU, whereas greater divergence is shown by a lower IoU.

$$\text{IOU} = \frac{Area\ of\ Overlap}{Area\ of\ Union} \qquad (5)$$

In this research, the IoU threshold is fixed at 0.7. In the context of object detection, when the overlap ratio between the region corresponding to the anchor frame and the true target area is greater than 0.7, it is typically considered a positive detection. This threshold is commonly used to determine whether an anchor (a predefined bounding box) accurately captures an object of interest in the image. Conversely, if the overlap ratio is less than 0.3, it will be considered a background region. Any regions that fall between the above two values are discarded or not considered during the detection process. As a result, the model requires less computing to operate, and runs faster, and the enhanced RPN generates less ROI, increasing the

model's effectiveness. Fig 4 shows the ROI generated from the proposed model.

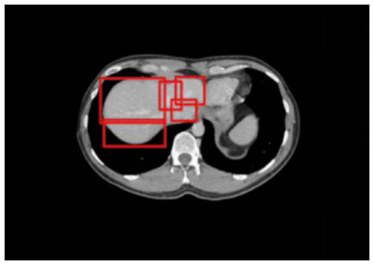

Fig 4. ROI generated by RPN

IV. EXPERIMENTS AND RESULTS

The suggested network was trained using a LiTS dataset [25] that is freely available to the public. A total of one hundred thirty Computed Tomography Scan volumes for training and seventy Computed Tomography Scan for testing make up the dataset. The datasets are provided by many clinical locations throughout the world and are publicly accessible on the LiTS challenge website. With a resolution of 0.6 mm in the plane and a slice thickness of 0.8 mm. Fig 5 shows sample images from the LiTS dataset.

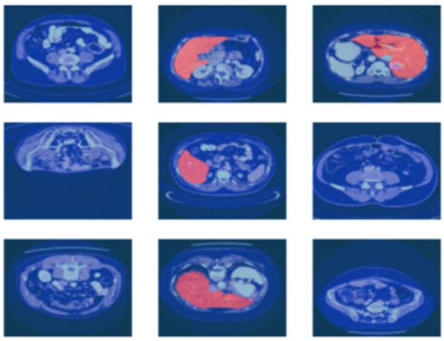

Fig 5: LiTs Dataset Images

Table 1 shows the experimental environments and major libraries which have been used in this research.The environment includes specifications and different software versions. The evaluation was held using TensorFlow with 16 GB RAM and NVIDIA GPU as shown.

Table 1. System Requirements

Component	**Requirement**
TensorFlow Version	2.10.0
Keras Version	2.2.4
RAM	16 GB
Processor	Intel i7-1065G7 CPU
GPU	NVIDIA GeForce GTX 1650ti
Operating System	Ubuntu 23.04 x86_64

Table 2. Parameter Settings

PARAMETERS	**VALUE**

Learning-Rate	0.001
Detection-minimum-confidence	0.7
Pool-size	7
Validation-Steps	50
Mask-Pool-Size	14
Steps-Per-Epoch	100
Num-Classes	2

Table 2 presents the various parameters that have been fixed after experimenting with various values and thresholds for the mask RCNN model. These parameters play an important role in the overall performance and behavior of the Mask R-CNN model during training and testing.

The following are the metrics used:

Accuracy: In equation 6 accuracy refers to the measure of correctly classified pixels or objects relative to the total number of pixels or objects in a given dataset or evaluation.

$$\text{Accuracy} = \frac{TP+}{TN+FP+TP+F} \quad (6)$$

Recall: Equation 7 demonstrates how well the framework can identify tumour pixels when compared to the total amount of real tumour pixels.

$$\text{Recall} = \frac{TP}{TP+FN} \quad (7)$$

Precision (Pr): As shown in equation 8 precision is calculated by dividing the true positive predictions (correctly identified cases) by the sum of the true positive and false positive predictions (cases predicted but are not).

$$\text{Precision} = \frac{TP}{TP+FP} \quad (8)$$

Dice Coefficient (F1 Score): As shown in equation 9 the dice coefficient is calculated by taking the harmonic mean of precision and recall.

$$\text{F1} = 2 * \frac{Pr*Re}{Pr+Re} \quad (9)$$

MIoU- The mIoU as shown in equation 10 is the mean of the IoU of the segmented objects over all of the test dataset's pictures.

$$\text{MIOU} = \frac{1}{k+1}\sum_{i=1}^{k}\frac{p_{ii}}{\sum_{j=0}^{k}p_{ij}+\sum_{j=0}^{k}p_{ji}-p_{ii}} \quad (10)$$

In the given context, k represents the total number of output classes. The variables pij, pji, and pii represent different counts of pixels based on their classification results.

- pij tells the total count of pixels that go with category i but are wrongly predicted or misclassified as category j.
- pji tells the total count of pixels that go with category j but have been wrongly predicted or misclassified as category i.
- pii tells the total count of pixels that are correctly classified and belong to category i.

The results obtained from the proposed method were extremely promising,which has been shown in Fig 6 showcasing exceptional performance.

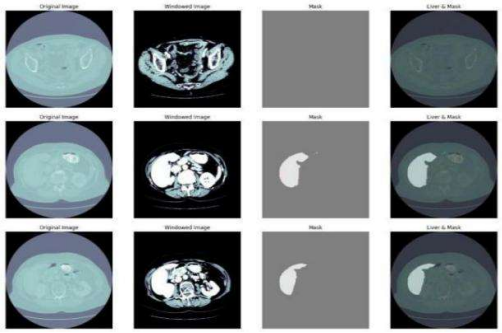

Fig 6. Liver Tumour Segmentation Results

Table 3. Comparative Analysis of the Proposed model

Model	**Accuracy**	**Precision**	**Recall**	**F1**	**MIoU**
CNN[22]	93.70	99.89	92.48	94.37	61.52
RNN[23]	81.26	99.41	74.63	87.58	73.79
GAN-RCNN [24]	92.43	99.78	91.53	95.86	81.25
MASK RCNN	95.27	99.93	94.10	97.32	88.64

To understand the execution of the improved model on the liver tumour dataset, it is compared with other Mask RCNN algorithms and models. It is verified from Table 3 that the enhanced Mask RCNN model shows notable advancements in detection performance compared to other models of the Mask RCNN. The proposed model provides better results in both terms of accuracy and detection also considering the speed, it gives better and enhanced results. The proposed model of Mask RCNN shows an accuracy of 95.27% which is higher than all the rest of the model.

V. CONCLUSION

In conclusion, Mask R-CNN liver tumour identification has proved advantageous in the world of medical imaging. The accurate identification and localization of liver tumor are only possible by using the Mask RCNN framework. By enabling early diagnosis Mask RCNN offers an opportunity for automated and accurate tumour identification. A comprehensive report of liver tumor is possible due to region proposal networks, feature extraction, and mask construction features of the Mask RCNN model. The architecture can also be adjusted and improved to accommodate various imaging modalities, such as CT, MRI, or ultrasound.

Mask RCNN is effective in detecting liver tumor, reaching high sensitivity and accuracy in several investigations. It helps radiologists and doctors make educated judgments, which improves the outcomes by detecting exact tumour boundaries. However, problems like dataset size, annotator quality, and computational needs still exist.

REFERENCES

[1] Christ, P.F., Elshaer, M.E., Ettlinger, F., Tatavarty, S., Bickel, M., Bilic, P., Rempfler, M., Armbruster, M., Hofmann, F.O., D'Anastasi, M., Sommer, W.H., Ahmadi, S., & Menze, B.H. (2016). Automatic Liver and Lesion Segmentation in CT Using Cascaded Fully Convolutional Neural Networks and 3D Conditional Random Fields. ArXiv, abs/1610.02177.

[2] Rahman H, Bukht TFN, Imran A, Tariq J, Tu S, Alzahrani A. A Deep Learning Approach for Liver and Tumor Segmentation in CT Images Using ResUNet. Bioengineering (Basel). 2022 Aug 5;9(8):368. doi: 10.3390/bioengineering9080368. PMID: 36004893; PMCID: PMC9404984.

[3] Rahman H, Bukht TFN, Imran A, Tariq J, Tu S, Alzahrani A. A Deep Learning Approach for Liver and Tumor Segmentation in CT Images Using ResUNet. Bioengineering (Basel). 2022 Aug 5;9(8):368. doi: 10.3390/bioengineering9080368. PMID: 36004893; PMCID: PMC9404984.

[4] Chen, L., Song, H., Wang, C. et al. Liver tumor segmentation in CT volumes using an adversarial densely connected network. BMC Bioinformatics 20 (Suppl 16), 587 (2019). https://doi.org/10.1186/s12859-019-3069-x

[5] Khoshkhabar, Maryam, Saeed Meshgini, Reza Afrouzian, and Sebelan Danishvar. 2023. "Automatic Liver Tumor Segmentation from CT Images Using Graph Convolutional Network" Sensors 23, no. 17: 7561. https://doi.org/10.3390/s23177561.

[6] Nisa, Mehrun, Saeed Ahmad Buzdar, Khalil Khan, and Muhammad Saeed Ahmad. 2022. "Deep Convolutional Neural Network Based Analysis of Liver Tissues Using Computed Tomography Images" Symmetry 14, no. 2: 383. https://doi.org/10.3390/sym14020383.

[7] Chung, Sheng Hung, et al. "Liver Tumour Segmentation Using Triplanar Convolutional Neural Network: A Pilot Study." 10th International Conference on Robotics, Vision, Signal Processing and Power Applications. Springer, Singapore, 2019.

[8] Dong, X., Zhou, Y., Wang, L., Peng, J., Lou, Y., & Fan, Y. (2020). Liver Cancer Detection Using Hybridized Fully Convolutional Neural Network Based on Deep Learning Framework. IEEE Access, 8, 129889-129898.

[9] Heng Zhang, Kaiwen Luo, Ren Deng, Shenglin Li, Shukai Duan, "Deep Learning-Based CT Imaging for the Diagnosis of Liver Tumor", Computational Intelligence and Neuroscience, vol. 2022, Article ID 3045370, 7 pages, 2022. https://doi.org/10.1155/2022/3045370.

[10] Das, A., Das, P., Panda, S.S. et al. Detection of Liver Cancer Using Modified Fuzzy Clustering and Decision Tree Classifier in CT Images. Pattern Recognit. Image Anal. 29, 201–211 (2019). https://doi.org/10.1134/S1054661819020056.

[11] Li, D.; Liu, L.; Chen, J.; Li, H.; Yin, Y. A multistep liver segmentation strategy by combining level set based method with texture analysis for CT images. In Proceedings of the 2014 International Conference on Orange Technologies, Xi'an, China, 20–23 September 2014; IEEE: Piscataway, NJ, USA, 2014; pp. 109–112.

[12] Xu, Z.; Burke, R.P.; Lee, C.P.; Baucom, R.B.; Poulose, B.K.; Abramson, R.G.; Landman, B.A. Efficient multi-atlas abdominal segmentation on clinically acquired CT with SIMPLE context learning. Med. Image Anal. 2015, 24, 18–27.

[13] Song, X.; Cheng, M.; Wang, B.; Huang, S.; Huang, X.; Yang, J. Adaptive fast marching method for automatic liver segmentation from CT images. Med. Phys. 2013, 40, 091917.

[14] Maklad, A.S.; Matsuhiro, M.; Suzuki, H.; Kawata, Y.; Niki, N.; Satake, M.; Moriyama, N.; Utsunomiya, T.; Shimada, M. Blood vessel-based liver segmentation using the portal phase of an abdominal CT dataset. Med. Phys. 2013, 40, 113501.

[15] Peng, J.; Dong, F.; Chen, Y.; Kong, D. A region-appearance-based adaptive variational model for 3D liver segmentation. Med. Phys. 2014, 41, 043502.

[16] S.Subhra, S. Mishra, A. Alkhayyat, V. Sharma and V. Kukreja, "Climatic Temperature Forecasting with Regression Approach," 2023 4th International Conference on Intelligent Engineering and Management (ICIEM), London, United Kingdom, 2023, pp. 1-5, doi: 10.1109/ICIEM59379.2023.10166883.

[17] P.Shrivastava and V. Sharma, "Debunking the 5G Covid 19 Myth-A Comprehensive Review of 5G and its Implications in IoT," 2023 4th International Conference on Intelligent Engineering and Management (ICIEM), London, United Kingdom, 2023, pp. 1-6, doi: 10.1109/ICIEM59379.2023.10166358.

[18] M. Sen, K. Sharma, S. Mishra, A. Alkhayyat and V. Sharma, "Designing a Smart and Intelligent Ecosystem for Autistic Children," 2023 4th International Conference on Intelligent Engineering and Management (ICIEM), London, United Kingdom, 2023, pp. 1-5, doi: 10.1109/ICIEM59379.2023.10166057.

[19] T.Mohanty, A. Behera, S. Mishra, A. Alkhayyat, D. Gupta and V. Sharma, "Resumate: A Prototype to Enhance Recruitment Process with NLP based Resume Parsing," 2023 4th International Conference on Intelligent Engineering and Management (ICIEM), London, United Kingdom, 2023, pp. 1-6, doi: 10.1109/ICIEM59379.2023.10166169.

[20] A.Raj, A. Kumar, V. Sharma, S. Rani and A. K. Shanu, "Enhancing Security Feature in Financial Transactions using Multichain Based Blockchain Technology," 2023 4th International Conference on Intelligent Engineering and Management (ICIEM), London, United Kingdom, 2023, pp. 1-6, doi: 10.1109/ICIEM59379.2023.10166589.

[21] A. Srivastava, S. Samanta, S. Mishra, A. Alkhayyat, D. Gupta and V. Sharma, "Medi-Assist: A Decision Tree based Chronic Diseases Detection Model," 2023 4th International Conference on Intelligent Engineering and Management (ICIEM), London, United Kingdom, 2023, pp. 1-7, doi: 10.1109/ICIEM59379.2023.10167400.

[22] Kaur, A.; Chauhan, A.P.S.; Aggarwal, A.K. An automated slice sorting technique for multi-slice computed tomography liver cancer images using convolutional networks. Expert Syst. Appl. 2021, 186, 115686.

[23] Rela, M.; Nagaraja Rao, S.; Ramana Reddy, P. Optimised segmentation and classification for liver tumour segmentation and classification using opposition-based spotted hyena optimization. Int. J. Imaging Syst. Technol. 2021, 31, 627–656.

[24] Wei, X.; Chen, X.; Lai, C.; Zhu, Y.; Yang, H.; Du, Y. Automatic Liver Segmentation in CT Images with Enhanced GAN and Mask Region-Based CNN Architectures. BioMed Res. Int. 2021, 2021, 9956983.

[25] P. Bilic et al., "The Liver Tumor Segmentation Benchmark (LiTS)," Medical Image Analysis, vol. 84, p. 102680, 2023, doi: https://doi.org/10.1016/j.media.2022.102680.